Materials Science-Poland, 35(4), 2017, pp. 878-884
http://www.materialsscience.pwr.wroc.pl/
DOI: 10.1515/msp-2017-0111

DE GRUYTER OPEN

Optical properties of ZnCoO layers obtained by PLD method

P. POTERA[1,*], I. VIRT[2,1], G. WISZ[1], J. CEBULSKI[1]

[1]Faculty of Mathematics and Natural Sciences University of Rzeszow, Rzeszow, Poland
[2]Drogobych State Pedagogical University, Drogobych, Ukraine

Optical properties of the zinc-cobalt oxide (ZnCoO) layers manufactured at different process conditions have been investigated. ZnCoO layers were grown on sapphire and glass substrates by pulsed laser deposition (PLD) technique. The influence of growth conditions as well as post-growth annealing on the films transmission and gap energy was analyzed.

Keywords: *optical properties; ZnO; thin films*

1. Introduction

Over the last few decades, zinc oxide has been extensively investigated for its use in various industries and technologies: spintronics, laser diodes, light emitting diodes, varistors and sensors, surface acoustic wave devices and transparent electrodes for solar cells and displays [1–8].

ZnO exhibits many favourable properties, such as high chemical stability, wide band gap (above 3.3 eV), high exciton binding energy (near 60 meV), abundance in nature, and is also regarded as nontoxic, environment friendly and low cost [9–13].

Several different physical and chemical methods have been used to fabricate high-quality ZnO thin films: pulsed laser deposition [12], molecular beam epitaxy [14], metalorganic chemical vapor deposition [15], direct current and radio-frequency magnetron sputtering [16], spin coating [17], dip coating [18], electrodeposition [19], and spray pyrolysis [20].

Doping non-magnetic semiconductors with transition metals (e.g. Co or other ions such as Ti, V, Cr, Mn, Fe, Ni and Cu) leads to the production of diluted magnetic semiconductors (DMS) which are regarded as important materials for spintronic and photonic devices.

The research on ternary ZnCoO semiconductors has been greatly stimulated by the high Curie temperature for the ferromagnetic transition existing in bulk materials and found to be around 300 K [21]. As a consequence, ZnCoO could be a good candidate for practical applications in advanced spintronic devices.

The doped ZnO thin films have also applications as transparent conductors because they have low resistivity and good optical gap energy at low temperature and are transparent in visible region. There are many reports on ZnO thin films doped with different elements (Co, Al, V, Ga, Mg, Li, P, N, Ni, and In) [21–30]. ZnCoO films have been extensively studied in last years [31–34] because they exhibit high mobility, good optical transparency, good electrical conductivity, and can be produced at lower material cost. For better using various devices, optical properties of ZnCoO DMS have been a focus of study, for example in [35–39].

It was shown that the transmission spectra and optical band gap energy of pure ZnO layers strongly depend on growth conditions as well as post-growth treatment [12, 16, 18, 20]. In this work, a study of optical properties of ZnCoO thin films obtained by PLD method on sapphire or glass substrates before and after annealing have been studied.

*E-mail: ppotera@univ.rzeszow.pl

2. Experimental

The ZnCoO thin films on the sapphire substrate were obtained by PLD method in Drohobych State University by using KWO_4 laser with repetition rate of 20 pulse/min and pulse energy of 0.2 J under 10^{-5} Pa vacuum. The time of deposition was 30 min. The targets with compositions $Zn_{0.96}Co_{0.04}O$ and $Zn_{0.80}Co_{0.20}O$ were used. The detailed information about the samples is given in Table 1.

The ZnCoO layers on glass substrate were obtained by PLD using of Modular Platform PREVAC in Rzeszow University. Thin films were deposited on microscope glass substrates (25 mm × 25 mm × 0.1 mm). The distance between the source and substrate was 2.6 cm. The YAG:Nd laser beam (second harmonic 532 nm) was focused on the target using a quartz lens with a focal distance of 600 mm. The 6 ns pulse time, and 16 J/cm^2 fluence were used. The pressure during deposition was maintained at 1.16×10^{-6} Pa. Sputtering was done for 20 minutes (Table 1).

The transmission spectra of the thin films were recorded by CARY 5000 spectrophotometer. Additionally, the samples were isochronously annealed in air (NABERTHERM LH04 furnace) at different temperatures (Table 1). After each annealing step (after cooling the sample) the transmission spectra were recorded.

3. Results and discussion

The transmissions spectra of the as-grown ZnCoO layers are given in Fig. 1.

The transmission spectra of the investigated samples strongly depend on growth conditions, target composition and substrate used. The samples No. 1 and 2 were grown at room temperature on sapphire substrate from a target with different Co content. The transmission of the sample obtained for 20 % Co content in the target is higher than that obtained for the target with 4 % Co content. The samples No. 3 to 5 were deposited on the glass substrates with higher temperatures (200 °C, 250 °C, 300 °C) from the target with 20 % Co content.

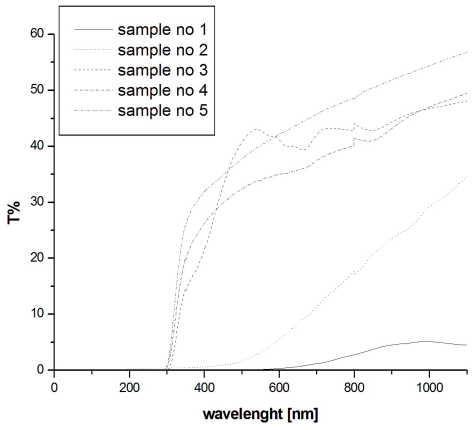

Fig. 1. Transmission spectra of the ZnCoO layers.

The transmission of these samples is significantly higher than for samples No. 1 and 2. For the sample No. 3, the characteristic d-d transitions in the tetrahedrally coordinated Co^{2+} [37, 40] (which replaces Zn^{2+} cations) were observed (Fig. 1), which suggests superior crystalline structure of this sample than of other samples.

The absorption edge of the investigated samples (Fig. 2) can be approximated by Tauc relation [41]:

$$\alpha h\upsilon = B(h\upsilon - Eg)^{\gamma} \tag{1}$$

where Eg is the optical band gap, h is the Planck constant, ν is the frequency of incident photons, B is a constant, and γ is the index, which can have different values (2, 3, 1/2 and 1/3) corresponding to indirect allowed, indirect forbidden, direct allowed and direct forbidden transitions, respectively. In our case, the approximation with $\gamma = 1/2$ was satisfactory for all samples, which corresponds to the direct allowed transitions observed earlier for pure ZnO layers [18].

For the direct transition, the optical band gap energy of the films was determined using the transformed equation 1:

$$(\alpha h\nu)^2 = A(h\nu - E_g) \tag{2}$$

Fig. 2 shows a graph $(\alpha h\nu)^2$ versus photon energy, allowing us to assess the value of the energy gap with a sharp absorption edge using linear approximation. The obtained values of E_g are given

Table 1. The sample characterizations.

No	Target	Tempearture of the substrate	Growth conditions	Substrate	Post-growth treatment
1	$Zn_{0.96}Co_{0.04}O$	30 °C	Deposition time 30 min, KWO_4 laser $\lambda = 1.064$ nm, repetition rate 20 pulse/min, power 0.2 J, vacuum 10^{-5} Pa	sapphire	Heating for 5 min at temperature 200 °C, 300 °C, 400 °C consecutively
2	$Zn_{0.8}Co_{0.2}O$	30 °C	Deposition time 30 min, KWO_4 laser $\lambda = 1.064$ nm, repetition rate 20 pulse/min, power 0.2 J, vacuum 10^{-5} Pa	sapphire	Heating for 5 min at temperature 550 °C, 700 °C, consecutively
3	$Zn_{0.8}Co_{0.2}O$	200 °C	Deposition time 20 min II harmonic YAG Nd, frequency 20 Hz, pressure 1.16×10^{-6} Pa	glass	Heating for 10 min at temperature 150 °C, 300 °C, 450 °C consecutively
4	$Zn_{0.8}Co_{0.2}O$	250 °C	Deposition time 20 min II harmonic YAG Nd, frequency 20 Hz, pressure 1.16×10^{-6} Pa	glass	Heating for 10 min at temperature 150 °C, 300 °C, 450 °C consecutively
5	$Zn_{0.8}Co_{0.2}O$	300 °C	Deposition time 20 min II harmonic YAG Nd, frequency 20 Hz, pressure 1.16×10^{-6} Pa	glass	Heating for 10 min at temperature 150 °C, 300 °C, 450 °C consecutively

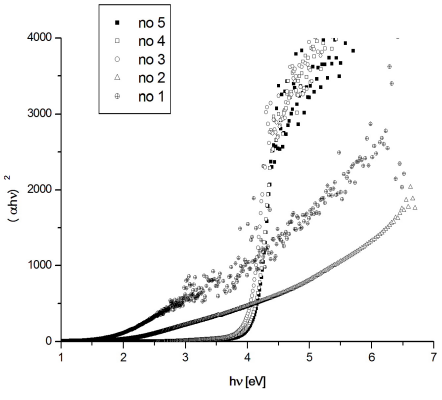

Fig. 2. Absorption of the samples in Tauc coordinates.

in Table 2. The values of E_g given in literature are 3.55 eV for a film deposited on a glass substrate and 3.3 eV to 3.8 eV for a film deposited on sapphire [32, 39, 40].

In the literature [12] it was shown that an increase in the optical energy gap with an increase of deposition temperature takes place in pure ZnO. This effect can partially explain the difference between the values of E_g for the samples. This increase in the energy gap is consistent with the considerable shift in Burstein electron density [12]. Unfortunately, sample 4 was obtained at a temperature higher than sample 3 but its energy gap is smaller. In the literature [40] it was shown, that the energy gap of ZnCoO increases with increasing cobalt concentration in the layer. This effect could be responsible for the differences in E_g values for samples No. 3 to 5 deposited on the same substrate with the same thickness.

The annealing of the sample No. 1 in air leads to the growth of transmission of this sample (Fig. 3).

Table 2. The E_g value for investigated samples.

Sample No. 1	Sample No. 2	Sample No. 3	Sample No. 4	Sample No. 5
1.96 eV	2.98 eV	4.03	3.85	4.16

The transmission value strongly depends on temperature of annealing.

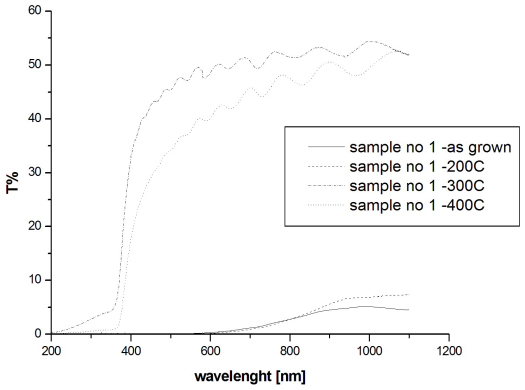

Fig. 3. The transmission spectra of sample No. 1 before and after annealing.

Annealing of sample No. 1 at temperature of 200 °C resulted in small transmission changes in comparison to the higher temperatures of annealing (300 °C, 400 °C). The annealing of sample No. 1 at temperature of 300 °C (Fig. 3) as well as sample No. 2 at temperature of 500 °C (Fig. 4) caused a radical increase of the average transmission value. The small transmittance of the samples which were grown at low substrate temperature can be due to the presence of Zn particles together with ZnO in the layers. The post-growth annealing can lead to oxidation of Zn and producing of the ZnO particles. This mechanism can also explain the significant change of E_g after heating. We also note that the fine-polycrystalline structure of our samples was found before heating. After annealing, the coarse-grained polycrystalline structure was detected by TEM method. Such changes can partially affect the increase in the transmission [20].

For annealing at the temperatures of 300 °C and 400 °C, a strong shift of absorption edge to the short wavelengths was observed for sample No. 1 in comparison to the no annealing state and the sample annealed at 200 °C. So, we can state that annealing strongly affected the value of optical energy gap of the layers (Table 3). The same remark concerns the sample No. 2. We note, that transmission of this sample practically has not changed after the growth of annealing temperatures from 500 °C to 700 °C (Fig. 4).

Table 3. E_g values for sample No. 1 and No. 2 for different annealing temperatures.

Sample No. 1		Sample No. 2	
Temperature of annealing	Eg [eV]	Temperature of annealing	Eg [eV]
before annealing	1.96	before annealing	2.98
200 °C	2.21	500 °C	3.52
300 °C	3.81	700 °C	3.57
400 °C	3.46		

The growth of transmission after annealing in air was also observed for other ZnCoO samples (Fig. 5 to Fig. 7). The increase of the transmission after annealing in air has already been observed for ZnO layers [12, 20]. We note, that Nadarajah et al. [20] showed that transmission of ZnO films increases with annealing temperatures due to the increase in grain size, structural homogeneity, and crystallinity. In our earlier work [12] we postulated that the increase in the optical transmission of ZnO layers after annealing in air can be associated with a decrease in oxygen defects.

Table 4. The E_g value for sample No. 3 to 5 for different annealing temperatures.

Temperature of annealing	Sample No. 3	Sample No. 4	Sample No. 5
	Eg[eV]		
before annealing	4.03	3.85	4.16
150 °C	4.05	3.88	4.16
300 °C	4.05	3.91	4.17
450 °C	4.07	3.93	4.17

For sample No. 3, the annealing in air practically has not influenced the optical energy gap.

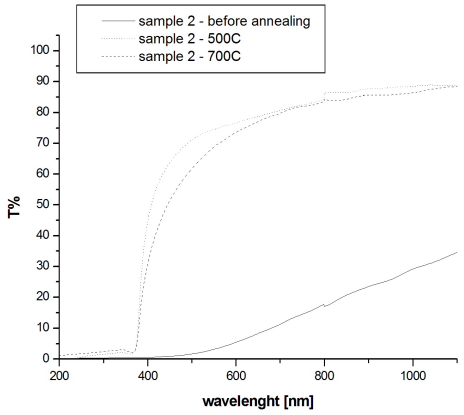

Fig. 4. The transmission spectra of sample No. 2 before and after annealing.

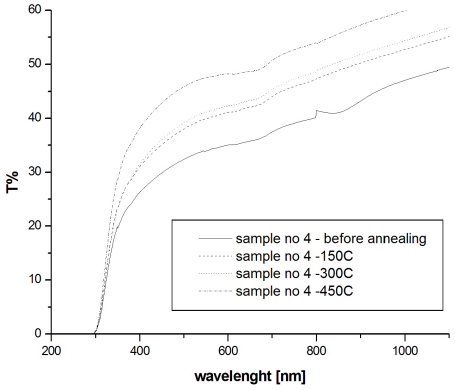

Fig. 6. The transmission spectra of sample No. 4 before and after annealing.

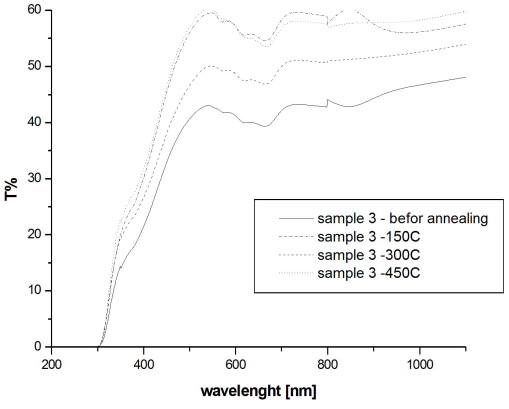

Fig. 5. The transmission spectra of sample No. 3 before and after annealing.

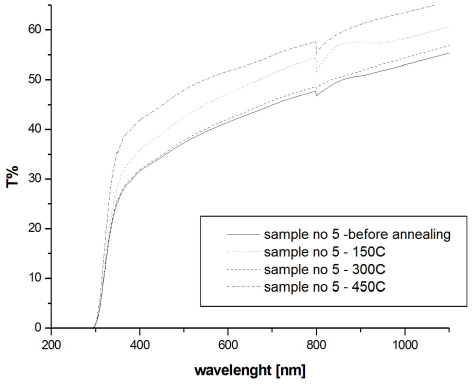

Fig. 7. The transmission spectra of sample No. 5 before and after annealing.

After each step of annealing, the E_g only slightly increased (Table 4).

For determination of activation energy E_a for absorption changes during annealing process, the dependencies of transmittance T at 800 nm as a function of annealing temperature T_{an} in Arhenius coordinates were drawn.

In Fig. 7 an example approximation is presented. The linearization was performed using equation:

$$lnT = B + (-E_a/(1000k) \cdot 1000/T_{an}) \qquad (3)$$

where k is the Boltzmann constant, E_a is an activation energy, B is a constant.

Equation 3 is a linear function of the type $y(x) = ax + b$, where $y = \ln(T)$, $x = 1000/T_{an}$ and $a = -E_a/(1000k)$. The approximation of the experimental data has been performed using Microcal Origin 6.0. In this way, E_a is given as $E_a = -1000$ k·a. The values of activation energy E_a are given in Table 5.

4. Conclusions

The growth conditions as well as target composition strongly affect the transmission spectra

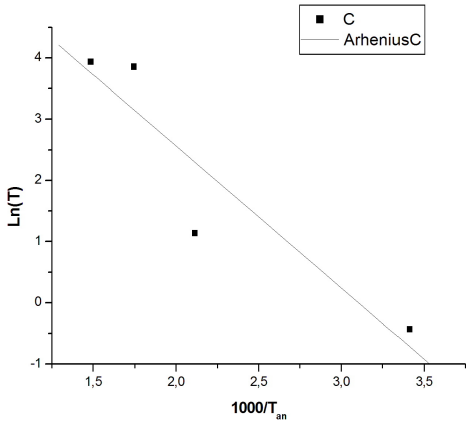

Fig. 8. The dependence of transmission of sample No. 1 at 800 nm versus temperature in Arheniuss coordinates.

Table 5. The E_a value for sample No. 3-4 for different annealing temperature.

Sample	No. 1	No. 2	No. 3	No. 4	No. 5
E_a [eV]	0.133	0.085	0.009	0.012	0.006

of ZnCoO layers and optical band gap energy of this material. The layers obtained at room temperature are poorly permeable, but for samples obtained at higher temperatures (200 °C to 300°C) a rather high transmittance was observed. The post-growth annealing in air resulted in an increase in the optical transmission for all investigated samples. Particularly high growth was observed for the samples obtained at room temperature. We also showed that the E_g value depends on the growth conditions and post-growth annealing.

References

[1] ÖZGÜR Ü., ALIVOV YA.I., LIU C., TEKE A., RESHCHIKOV M.A., DOĞAN S., AVRUTIN V., CHO S.-J., MORKOÇ H., *J. Appl. Phys. 98*, (2005) 041301.

[2] KHRANOVSKYY V., ERIKSSON J., LLOYD-SPETZNITA A., YAKIMOVA R., HULTMAN L., *Thin Solid Films* 517, (2009) 2073.

[3] LORITE I., RUBIO-MARCOS F., ROMERO J.J., FERNÁNDEZ J.F., *Mater. Lett.*, 63, (2009) 212.

[4] PHAN T.L., SUN Y.K., VINCENT R., CHERNS D., NGHIA N.X., YU S.C., *J. Korean. Phys. Soc.*, 52, (2008) 1633.

[5] RYU Y.R., LEE T.S., LUBGUBAN J.A., WHITE H.W., PARK Y.S., YOUN C.J., *Appl. Phys. Lett.*, 87, (2005) 153504.

[6] NGAN P.H., TIEN N.Q., DAT D.T., NHO P.V., NGHIA N.X., YU S.C., *J. Korean. Phys. Soc.*, 52, 1594 (2008).

[7] GIRIJA K.G., SOMASUNDARAM K., TOPKAR A., VATSA R.K., *J. Alloy Comp.*, 684(5) (2016), 15.

[8] YA K.X., YIN H., DE T.M., JING T.M., *Mater Res Bull*, 33, (1998) 1703.

[9] LEE J.H., KO K.H., PARK B.O., *J. Cryst. Growth*, 247(1 – 2), (2003)119.

[10] KONENKAMP R., BOEDECKER K., LUX-STEINER M., POSCHENRIEDER C. M., ZENIA F., LEVY-CLEMENT C., WAGNER S., *Appl. Phys. Lett.*, 77(16), (2000) 2575.

[11] VIRT I.S., HADZAMAN I.V., BILYK I.S., RUDYI I.O., KURILO I.V., FRUGYNSKYI M.S., POTERA P., *Acta Phys. Pol. A*, 117(1), (2010) 34.

[12] WISZ G., VIRT I., SAGAN P., POTERA P., YAVORSKYI R., *Nanoscale Res. Lett.*, 12, (2017) 253.

[13] SINGH S., KAUR H., PATHAK D., BEDI R.K., *J. Nanomater. Bios.*, 6(2), (2011), 689.

[14] LOOK D.C., REYNOLDS D.C., LITTON C.W., JONES R.L., EASON D.B., CANTWELL G., *Appl. Phys. Lett.*, 81(10), (2002) 1830.

[15] TAN S.T., CHEN B.J., SUN X.W., FAN W.J., KWOK H.S., ZHANG X.H., CHUA S.J., *J. Appl. Phys.*, 98, (2005) 013505.

[16] CHO S., *Trans. Electr. Electron. Mat.* 10(6), (2009) 185.

[17] SRINIVASAN G., GOPALAKRISHNAN N., YU Y.S., KESAVAMOORTHY R., KUMAR J., *Superlattice Microst.*, 43(2), (2008) 112.

[18] KAYANI Z.N., QBAL M., RIAZ S., ZIA R., NASEEM S., *Mat. Sci.-Poland*, 33(3), (2015), 515.

[19] DALCHIELE E. A., GIORGI P., MAROTTI R. MARTIŃE F., AYOUCI R., LEINEN D., *Solar Energ. Mat. Sol. C.*, 70(3), (2001) 245.

[20] NADARAJAH K., CHEE C.Y., TAN C.Y., *J. Nanomater.*, (2013), 1 (Article ID 146382).

[21] DIETL T., OHNO H., MATSUKURA F., *Phys. Rev. B* 63, (2001) 195205.

[22] BENRAMACHE S., BENHAOUA B., CHABANE F., *J. Semicond.* 33, (2012) 093001–1

[23] YAMADA T., NEBIKI T., KISHIMOTO S., MAKINO H., AWAI K., NARUSAWA T., YAMAMOTO T., *Superlattice. Microst.*, 42, (2007) 68.

[24] DUCLÈRE, J.R., NOVOTNY M., MEANEY A., O'HAIRE R., MCGLYNN E., HENRY M.O., MOSNIER P.J., *Superlattice. Microst.*, 38 (2005), 397.

[25] ABED S., AIDA M.S., BOUCHOUIT K., ARBAOUI, A., ILIOPOULOS K., SAHRAOUI B., *Opt. Mater.*, 33, (2011) 968.

[26] BENRAMACHE S., BENHAOUA B., *Superlattice. Microst.*, 52, (2012) 807.

[27] BENRAMACHE S., BENHAOUA B., BENTRAH H., *J. Nanostr. Chem.*, 3 (2013) 54.

[28] RIVERA M.J., RAMÍREZ E.B., JUÁREZ B., GONZÁLEZ J., GARCÍA-LEÓN J.M., ESCOBAR-ALARCÓN L., ALONSO J.C., *Thin Solid Films*, 605, (2016), 108.

[29] SUZUKI T., CHIBA H., KAWASHIMA T., WASHIO K., *Thin Solid Films*, 605, (2016), 53.
[30] HORNG R.H., OU S.L., HUANG C.Y., RAVADGAR P., WU C.I., *Thin Solid Films 605*, (2016), 30.
[31] TYPEK J., GUSKOS N., ZOLNIERKIEWICZ G., SIBERA D. NARKIEWICZ U., *Rev. Adv. Mater. Sci.*, 50 (2017) 76.
[32] KAYANIA Z. N., AFZALA A., KHANA E. S., NAZIRA F., SALEEMIA F., RIAZB S., NASEEMB S., *Materials Today: Proceedings*, 2 (2015) 5473.
[33] SU Y.L., ZHANG Q.Y., ZHOU N., MA C.Y., LIU X.Z., ZHAO J.J., *Solid State Commun.*, 250, (2017), 123.
[34] ZENG Y., GAUQUEL N, LI D., RUAN S, HE H., EGOAVIL R., YE Z., VERBEECK Y., HADERMANN J., BAEL M.J., HAESENDONCK CH, *ACS Appl. Mater. Inter.*, 40 (2015), 22166.
[35] WOLSKA E., ŁUKASIEWICZ M., FIDELUS J.D, ŁOJKOWSKI W., GUZIEWICZ, GODLEWSKI M., *Acta Phys. Pol.*, 116(5), (2009) 918.
[36] CAO P., BAI Y., *Advanced Materials Research*, 781-784 (2013), 323.
[37] TORTOSA M., MOLLAR M., MARÍ B., LLORET F., *J. Appl. Phys.*, 104 (2008), 033901.
[38] LI C., GAO G., CHEN X., *MATEC Web of Conferences*, 67, (2016) 02004
[39] VUICHYK M.V., TSYBRII Z.F., LAVORYK S.R., SVEZHENTSOVA K.V., VIRT I.S., CHIZHOV A., *Semicond. Phys., Quant. El. Optoelectron.*, 17 (2014), 80.
[40] IVILL M., PEARTON S.J., RAWAL S., LEU L., SADIK P., DAS R., HEBARD A.F., CHISHOLM M., BUDAI J.D., NORTON D.P., *New J. Phys.*, 10 (2008) 065002.
[41] VIEZBICKE B.D., PATEL S., DAVIS B.E., BIRNIE D.P., *Phys. Status Solidi B*, 252(8) (2015), 1700.

Received 2017-07-10
Accepted 2017-12-14